Experimental and Numerical Characterization of an Ablation-fed Pulsed Plasma Thruster Prototype

IEPC-2009-246

Presented at the 31st International Electric Propulsion Conference,
University of Michigan, Ann Arbor, Michigan, USA
September 20–24, 2009

Erik M. Henrikson* and Pavlos G. Mikellides †
Arizona State University, Tempe, Arizona, 85287

Hani Kamhawi‡
NASA Glenn Research Center, Cleveland, Ohio, 44135

A traditionally configured ablation-fed pulsed plasma thruster (APPT) operating between 40 and 140 Joules was modeled using the computational magnetohydrodynamic tool MACH2 in order to validate a simplified ablation model based on an energy-flux balance at the surface of a solid propellant, polytetrafluoroethylene (PTFE). The simulated total ablated mass corresponded to experimental mass loss data to within 15%. MACH2 and the simplified ablation model were then used to model a novel APPT configuration, providing insight into discharge behavior in an APPT of such geometry. Experimental results of ablated mass and current waveform for this geometry operating at 60 joules were obtained at two separate facilities and compared to the computational results, providing further validation of the ablation model and establishing a baseline for future optimization of alternative configurations.

Nomenclature

A = Area of Propellant Face
h = Height of Discharge Channel
h_{vap} = Propellant Heat of Vaporization
I_{bit} = Impulse Bit
J = APPT Circuit Current
j = Current Density
$\dot{m}$ = Mass Flow Rate
m_{abl} = Ablated Mass per Discharge
μ_o = Permeability of Free Space
q_i = Incident Heat Rate to Propellant Face
q_i'' = Incident Heat Flux to Propellant Face
q_r = Radiative Heat Rate
q_s'' = Heat Flux into Solid
ρ_i = MACH2 Inlet Density
u_g = Velocity at Propellant Surface
u_i = MACH2 Inlet Velocity
V_{crit} = Alfvén Critical Speed
w = Width of Discharge Channel

*Graduate Research Assistant, School of Mechanical, Aerospace, Chemical and Materials Engineering (MACME), Erik.Henrikson@asu.edu
†Associate Professor, CTI Department of Engineering, Polytechnic Campus, Pavlos.Mikellides@asu.edu
‡Research Engineer, Propulsion and Propellants Branch, 21000 Brookpark Rd/Ms 301-3, Hani.Kamhawi-1@nasa.gov

I. Introduction

Ablation-fed pulsed plasma thrusters (APPTs) are conceptually some of the simplest electromagnetic propulsion devices conceived, which make them extremely attractive due the resulting reduced mass and cost. The use of a solid propellant, typically polytetrafluoroethylene (PTFE), eliminates the complexities of gas-feed systems and simplifies propellant storage and handling during spacecraft integration. The technology dates back to the 1960's,[1] including a successful flight heritage demonstrated most recently by the Air Force Academy's FalconSat-3 mission. An APPT propulsion system is ideal for micro- and nano-satellite applications due to its potential for high specific impulse (∼1000s) and precision pointing capability, making it an excellent candidate for Earth and Space science missions including orbit insertion, orbit maintenance, and attitude control. Figure 1 displays the APPT in its traditional, breech-fed configuration. Energy is provided by a capacitor that discharges within a few microseconds across the face of the solid propellant. The discharge across the electrodes vaporizes and ionizes a portion of the solid propellant which in turn is primarily accelerated by the Lorentz electromagnetic force.

Despite the various advantages, the overall efficiency of the APPT is very low, limiting its application aboard various missions. The main factors causing inefficient operation stem from poor propellant utilization and acceleration. Many efforts have been made experimentally which have explored thruster geometry, current waveform, and propellant composition in attempts to overcome some of the thrusters inherent drawbacks.[1] There have also been a number of studies modeling the APPT's operation both analytically and numerically.[2–5] The results of such studies all express the significant impact that mass utilization and time scales have on an APPT's efficiency.

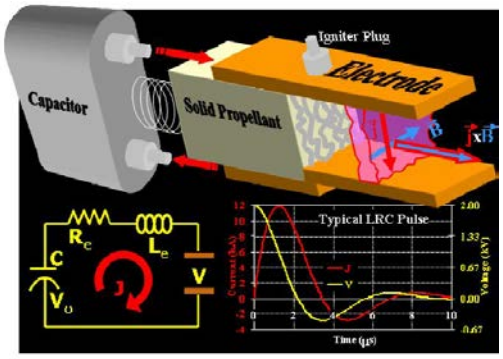

Figure 1. APPT in traditional rectangular configuration with representative circuit and current/voltage waveforms.

Modeling the physical processes of APPT operation utilizing numerical and computational means provides an efficient avenue to explore specific complexities present during operation, as well as a way to experiment with and optimize various APPT configurations. In an effort to develop such a simulation tool, a simplified ablation model has been implemented in the MHD code MACH2, and validated with respect to predicting total ablated mass during an APPT discharge. This model is then used to simulate a new APPT geometry which looks to enhance propellant utilization by imposing a physical restriction on the discharge current, forcing the discharge to remain behind the propellant throughout the entire current pulse. Such a configuration may allow the majority of the ablated mass to be accelerated to high exhaust speeds by the upstream electromagnetic forces, either directly or via collisions between ions and neutrals. The new geometry has also been fabricated and operated at two different facilities, aiding in validation of the computational model and verifying its experimental behavior.

II. APPT Computational Model

A. The MACH2 MHD Code

The 2-1/2 dimensional Multi-block Arbitrary Coordinate Hydromagnetic code (MACH2) is a time-dependent, multi-material MHD code that can be applied to problems of complex geometries due to its multi-block structure. It has successfully modeled various electromagnetic devices, including pulsed inductive thrusters,[6] MPD Arcjects,[7] and APPTs[2] in the past. A finite-volume spatial differencing scheme is used to time advance the single-fluid MHD equations and the boundary conditions are applied via ghost cells at the boundaries. The equations for mass continuity and momentum are solved assuming a single compressible fluid, but MACH2 solves two energy equations allowing for situations where the ions and electrons are in thermal non-equilibrium. Evolution of the magnetic field is determined by the magnetic induction equation that includes resistive diffusion with various models for the plasma resistivity.

An analytic or tabular equation of state completes the full set of MHD-equations. The tabular equation of state is implemented in MACH2 via the SESAME library,[8] which includes semi-empirical models for

the thermodynamic properties and average ionization state under local thermodynamic equilibrium (LTE). MACH2 is also capable of implementing various circuit models such as pulse forming networks, LRC circuits, and sine waveforms.

B. Ablation Model

In previous numerical studies, the ablation process of solid PTFE propellant has been handled in various ways. One such approach utilizes the equilibrium vapor pressure of the propellant based on the surface temperature as a boundary condition for the density at the ablating surface.[4,9] The surface temperature in this case is calculated by solving the two-dimensional diffusion equation within a semi-infinite solid. One potential drawback of this approach is the highly exponential behavior of the vapor pressure curve, which may lead to significant sensitivity due to small changes or error in the surface temperature calculation. Another approach implements a zero-dimensional analytic model utilizing conditions of the overall flow field through the evaluation of flow properties at both magnetosonic and sonic points of flow in a channel.[5,10] This model assumes the flow to be quasi-steady, of high magnetic Reynolds number, and magnetic pressure much greater than the plasma pressure. This method predicts a mass flow rate that scales with the square of the discharge current, given by the relation

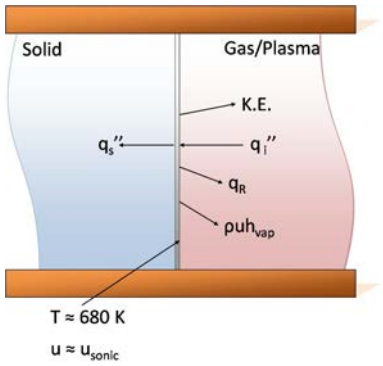

Figure 2. Schematic of energy flux balance at the propellant surface

$$\dot{m}(t) = \frac{\mu_o h J^2(t)}{w V_{crit} 4.404} = \alpha J(t)^2 \tag{1}$$

where α is a constant. Though this method has previously captured general trends in ablated mass for traditionally configured APPTs,[10] it is limited to cases where the flow is one dimensional.

An approximate method can be formulated through an energy-flux balance at the surface of the ablating propellant (fig. 2) which does not depend on a highly exponential expression and is not limited to one-dimensional channel flows. In general, the energy-flux balance defining the boundary condition at the surface of the propellant neglecting radiative losses can be written as

$$q_i'' = q_s'' + \frac{\dot{m}}{A}\left(\frac{u_g^2}{2} + h_{vap}\right) \tag{2}$$

If it is assumed that the right hand side of eq. 2 is dominated by the energy required to vaporize the propellant, a simple expression can be written that expresses the mass flow rate of the gas vaporized from the PTFE face in terms of the incident heat flux at the surface of the propellant. This expression is given as

$$\dot{m} = \frac{q_i}{h_{vap}}. \tag{3}$$

Recognizing that the value of q_i is going to be governed by joule heating, ηj^2, eq. 3 resembles the direct proportionality of mass flow rate to current described by eq. 1 in cases where it can be assumed that the resistivity remains relatively constant.

This model is implemented in the MACH2 by rewriting eq. 3 to express density in terms of heat flux, inlet velocity, and heat of vaporization. This expression is then used by MACH2 for the inflow density boundary condition at the surface of the propellant. This expression is given as

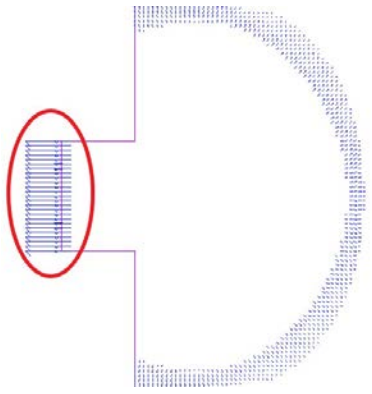

Figure 3. MACH2 thermal flux vector distribution across the ablating surface at 1 μs

$$\rho_i = \frac{q_i''}{u_i h_{vap}} \tag{4}$$

For this simplified model, it is assumed that the vaporized gas emanates at an effective decomposition temperature of 673K and that the propellant is immediately driven to sonic speeds, which for a molecular

gas of CF_2 is about 380 m/s.[11] The value used for the heat of vaporization of the solid PTFE in the following results was 2.11×10^6 J/kg.

The code is capable of solving for the thermal heat flux across an exterior boundary that is modeled as a thermal conductor. This capability is utilized to determine the last term in eq. 4, the incident heat flux at the surface of the propellant, q_i''. When implementing this model at the propellant surface, the condition on the temperature at the thermally conducting boundary is assumed to be the effective decomposition temperature of PTFE. The value of q_i'' in eq. 4 is then set to the average value of the thermal heat flux calculation over the ablating boundary from MACH2. For the breech fed configuration, this simple averaging of the flux can be justified by looking at uniformity of the heat flux distribution over the propellant surface, shown in fig. 3. For more complex geometries a more sophisticated approach may be necessary to fully capture the behavior of the ablation process.

C. Computational Setup

Two different APPT configurations were modeled using the MACH2 code utilizing the ablation model presented above. The results of this modeling are presented in the following sections. One of these configurations is a traditional, breech-fed APPT which has been experimentally characterized at NASA Glenn Research Center operating between 40J and 140J.[12] The thruster's electrodes are spaced 3.81 cm apart and are 2.54 cm wide with an electrode length in the thrust direction of 2.54 cm. The capacitance of the thruster's energy storage device is 48 μF.

The second configuration modeled an alternative geometry that places the ablating surface downstream of the discharge. In this manner, any portion of the ablated mass during the discharge that is not ionized may still benefit from electromagnetic acceleration in a snowplow fashion. This thruster's energy storage capacitance was 50 μF.

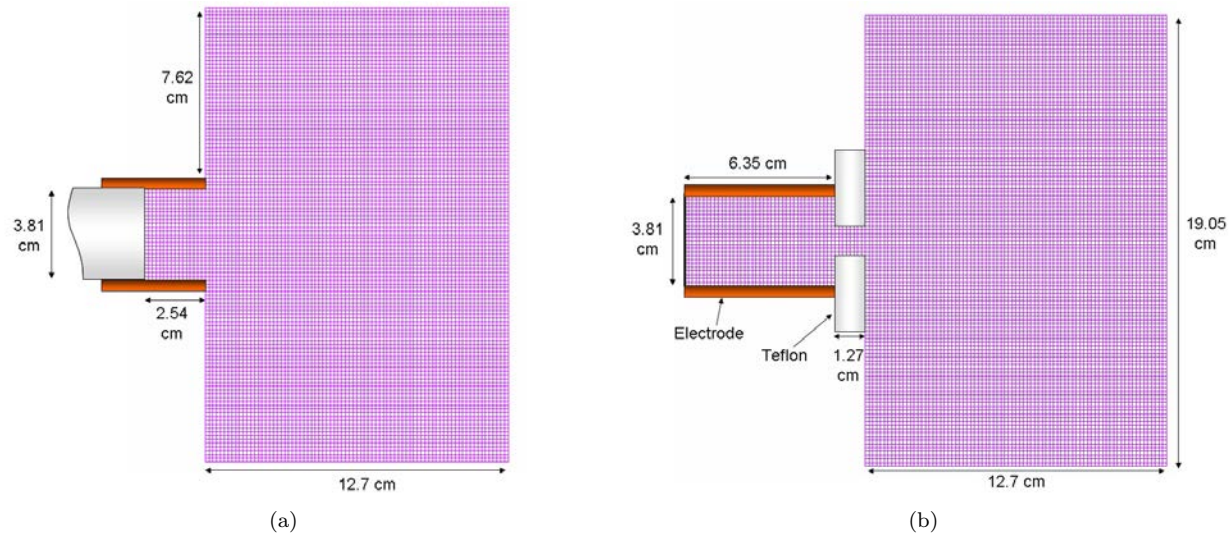

Figure 4. (a) Computational domain used for simulations of traditionally configured Glenn thruster (b) Computational domain used for simulations of prototype, PTFE spacing at exit is 1.27 cm

The electrodes for both cases were modeled as free-slip thermal insulators and magnetic conductors while the propellant surfaces were modeled as thermal conductors and magnetic insulators. The back plate for the novel configuration was modeled as a thermal and magnetic insulator. The computational domain extended well downstream of the of the thruster's exhaust region in order to fully capture the acceleration process and ensure that there was no influence from the outer boundaries where the flow property boundary conditions are modeled at zero gradient. The SESAME tabulated equation of state for PTFE, which includes a degree-of-ionization model assuming local thermodynamic equilibrium, was applied in the presented simulations. An LRC circuit model was implemented across the insulator face in order to match the experimental current waveform of each thruster operating at the respective energy levels. The initial global temperature and density were 300K and 1×10^{-7} kg/m^3, respectively. The thermal conductivity was characterized using the

Spitzer model, while the resistivity model includes contributions from electron-ion coulomb collisions as well as electron-neutral collisions.

III. Simulation Results

Simulations for the traditionally configured APPT were conducted over a simulation time of 50 μs for all energy levels, while the simulation times of the uniquely configured APPT were 250 μs. Though these times exceeded the discharge times, the length ensured that all mass had been expelled from the thruster through either electromagnetic or gas dynamic processes. All computational results utilized the simplified ablation model presented above. The simulated thrust was found by taking the integral of the dynamic pressure at the exhaust boundaries. This thrust was in turn integrated over the simulation time to provide impulse bit estimates. The resulting computations of impulse bit and ablated mass were investigated through comparison with available experimental data,[12] and are presented in figures 5(a) and 5(b) as well as table 1.

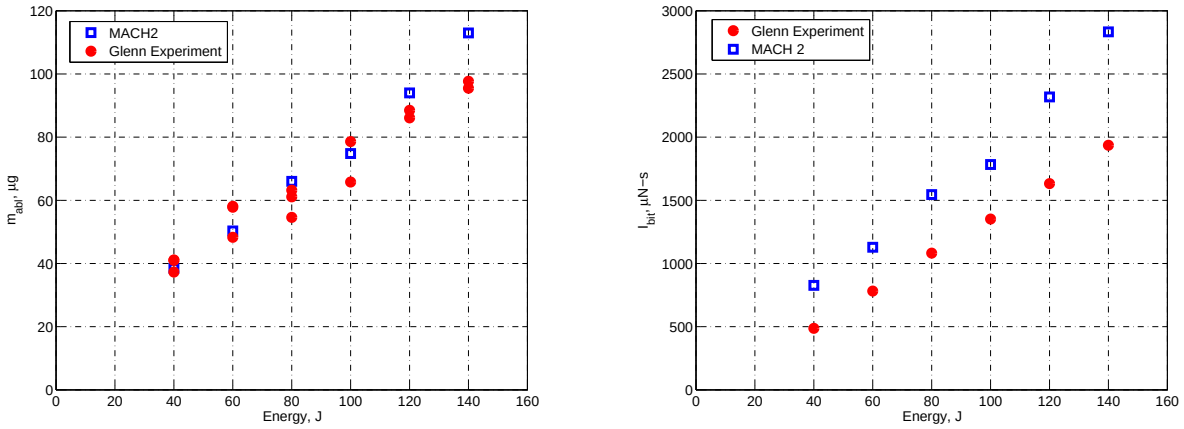

(a) (b)

Figure 5. Comparison of experimental and computational ablated mass (a) and impulse bit (b) for breech-fed NASA Glenn APPT

Table 1. Experimental and MACH2 Mass Loss and Impulse bit

Energy, J	Exp. Δm, μg	MACH2 Δm, μg	Exp. I_{bit}, μN-s	MACH2 I_{bit}, μN-s
40	41.0	38.5	486.9	827
60	54.7	50.3	781.5	1129
80	63.2	66.0	1082	1546
100	78.6	74.8	1352	1783
120	88.5	94.0	1632	2318
140	97.7	113	1936	2833

From the figures, it is apparent that the model captures a general trend in ablated mass, with a tendency to overpredict at the higher energy levels. This over prediction is most likely related to the ablation model assumptions that the chemical processes dominate the conversion of the incident heat flux. At higher energy levels a larger fraction of the incident heat flux may go into other modes such as heating of the remaining solid propellant and radiation.

The impulse bit predictions for these same results on average overpredict the experimental values by about 45%. A probable cause for a portion of this discrepancy is related to the current tabulated equation of state model for PTFE, which contains a limited range of density values and corresponding thermodynamic data.

This forces the code to extrapolate over a sizable range when dealing with lower density values. Due to this issue, energy deposition and ionization may not be properly captured, leading to significant discrepancies in computed average ionization state and kinetic energy. The possible shortcoming is currently being remedied by the construction of a more accurate and comprehensive thermochemical model.

Although the current model in MACH2 overpredicts the impulse bit, the agreement between experimental and predicted ablated mass for the energy levels being explored provides confidence in using the current modeling setup to qualitatively explore different APPT configurations in comparison to an established benchmark standard. This led to the modeling of the alternative configuration depicted in fig. 4(b) at an energy of 60J.

The current waveform implemented for the initial simulations was based on some preliminary experiments conducted at ASU. Once a housed prototype had been built and operated, this waveform was updated. The results presented in this paper for the alternative configuration were all found utilizing the updated waveform obtained from the formal prototype thruster presented in the following section. For these simulations, MACH2 predicted a total ablated mass of 186 μg and an impulse bit of 1261 $\mu N - s$. Figure 6 displays the resulting mass flow rate and discharge current over the length of the entire simulation.

These initial results for estimated impulse bit are only slightly higher than those computed for the breech-fed APPT operating at the same energy level, yet over three times the amount mass was lost. One interesting aspect of this result is the amount of mass that is lost from the face of the propellant after the discharge. From the simulations, it appears that almost a third of the propellant evaporates after the capacitor has completely discharged do to heat flux from the high temperature gas remaining between the electrodes. This gas was confined to the corners during the current pulse, hindering it from experiencing acceleration due to electromagnetic forces. Figures 7(a) and 7(b) display this confinement of the propellant at the corners by the current at 4 μs. Although a third of the mass is vaporized after the discharge, this hot gas still accounts for about a quarter of the total calculated impulse bit once allowed to exhaust from the thruster.

Comparisons of these computational results with experimentally obtained data from an APPT prototype of same geometry are presented in the following section.

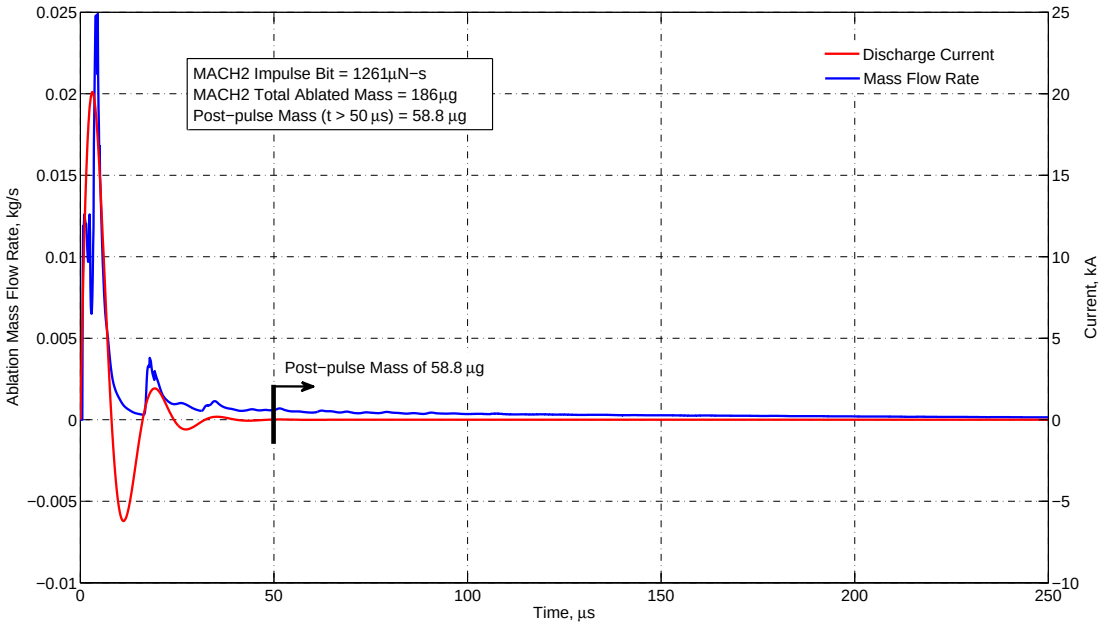

Figure 6. MACH2 combined mass flow rate from the faces of the ablating propellant and the discharge current waveform. The $58.8\mu g$ accounts for about a quarter of the total impulse bit.

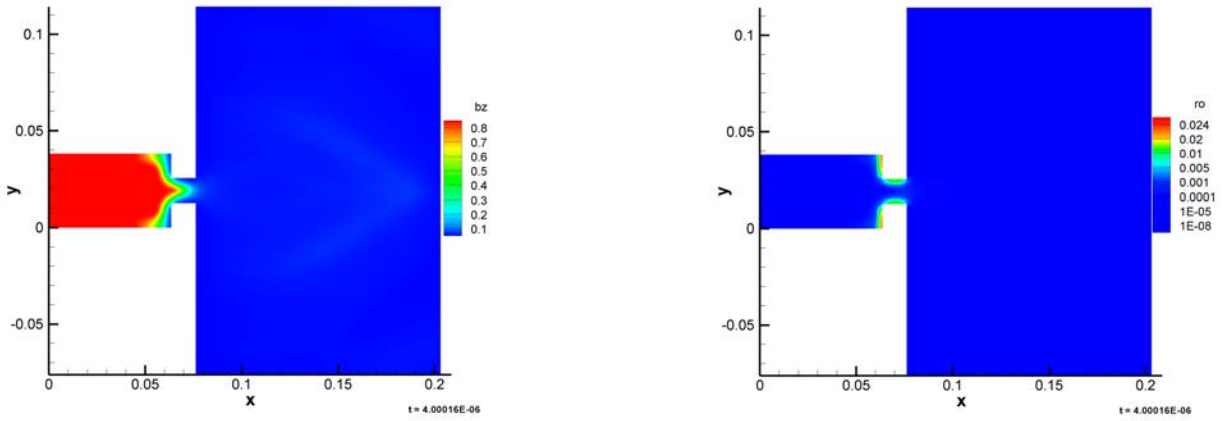

(a) $4\mu s$ (b) $4\mu s$

Figure 7. (a) Magnetic field in the z-direction signifying the current distribution at $t = 4\mu s$. (b) Distribution of density at $t = 4\mu s$.

IV. Experimental Characterization of Novel APPT Configuration

After conducting some preliminary simulations of the alternative APPT geometry, a physical prototype was designed and built in order to further validate the ablation model in MACH2 and provide a baseline for future optimization of alternative APPT designs. Once the prototype had been fabricated, experimental acquisition of current waveform and ablated mass were obtained for 60J operation at two separate facilities. The first of these facilities was located at Arizona State University in the Advanced Space Propulsion and Plasma Physics Lab (ASP^{3}L),[10] and the second at NASA Glenn Research Center (GRC).

A. Prototype APPT Thruster

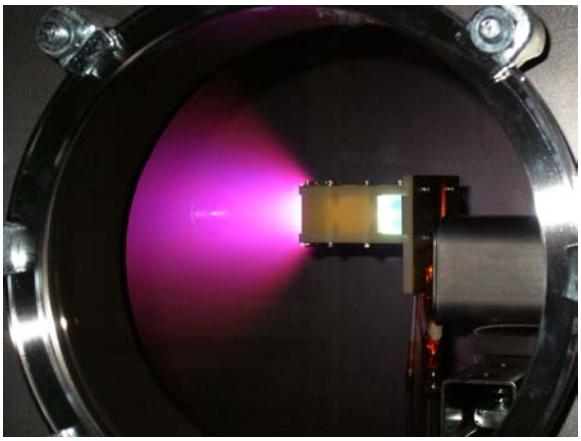

Figure 8. Prototype APPT during operation at the ASP^{3}L High Vacuum Facility

A prototype APPT that places the propellant downstream of the discharge, as is depicted in fig. 4(b), was designed and built at Arizona State University. This configuration is designed to allow the majority of the ablated mass to be electromagnetically accelerated regardless of its chemical composition, as all propellant can be swept by the upstream electromagnetic forces, either directly or via collisions between ions and neutrals. The energy storage device is a Maxwell 50 F, 2.0 kV, oil-filled capacitor, and the discharge between the two copper electrodes was initiated by a Unison turbine ignition circuit. This circuit consists of a Unison TGLN-28 igniter exciter, 1.27 cm ignition plug, and corresponding ignition lead. The ignition plug was embedded in the thruster cathode, which provided an electrical path between it and the plug cathode (shell). Pulse frequency during these tests was approximately 1 hertz. The transmission lines were machined from aluminum and the housing from Garolite (G-10).

B. Experimental Setup and Results

1. *Prototype Operation at the ASP^{3}L and NASA Glenn*

The two primary measurements taken at the ASP^{3}L High Vacuum Facility to initially characterize the prototype thruster were current waveforms and mass loss per discharge. The current waveform was obtained through the use of an in-house fabricated and calibrated Rogowski coil and the mass loss data was obtained by measuring the initial mass of the propellant, firing the thruster over a large number of pulses (∼3000), and then measuring the final mass. This total mass loss was then divided by the number of pulses in order to obtain the mass loss per pulse. The mass measurements were taken using a Mettler AE240 balance with a capacity of 40 g and a readability of 0.01 mg. The capacitor was charged using a Glassman 3 kV, 200mA high voltage power supply and the Rogowski coil output measured by a Tektronix TDS 540A, 4 channel, 500 MHz digitizing oscilloscope. Typical back pressure during operation was 1×10^{-6} Torr.

Figure 8 shows the APPT prototype firing at the ASU facility. Over three separate tests of 3000 pulses at 1 Hz, the average ablated mass was 149 μg. The obtained current waveform is shown in fig. 9.

Mass loss and current waveform data of the novel prototype operating at 60J were also obtained at NASA Glenn Research Center in Vacuum Facility 3 (VF3). The average back pressure during thruster operation was 5×10^{-6} Torr, which is slightly higher than the back pressure for the ASU tests. The value of ablated mass was quantified in the same manner as the tests in the ASU facility, with the exception of the number of pulses. The data from NASA GRC was obtained over ∼2300 discharges rather than 3000, while operating at the same frequency of 1 Hz. This resulted in a measured ablated mass per pulse of 157 μg. The average discharge current waveform is given in fig. 9 alongside the waveform acquired at ASU and the discharge current modeled in MACH2. Small discrepancies between the experimental values obtained at the separate facilities are most likely due to variations in operating environment as weel as other factors contributing to experimental variation. Overall, the results provide firm verification of the prototype's operational behavior allowing for further validation of the computational model.

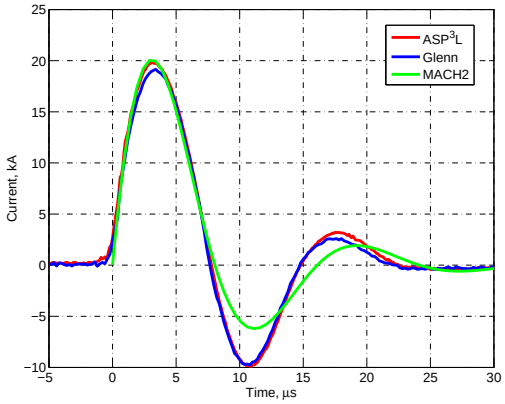

Figure 9. Novel configuration current waveforms acquired from both facilities obtained at 60J and the modeled waveform from MACH2.

2. *Comparison of Experimental Results with MACH2*

Comparing the ablated mass obtained from experiment to that calculated by MACH2, the computational results overpredict the mass loss value by about 20%. Aside from discrepancy due to the ablation models inherent assumptions, further discrepancy could be due to averaging the heat flux values over the ablating boundary which may not accurately capture the 2-D behavior of the prototype configuration. Future work includes upgrading the present model to capture this behavior for each computational cell rather than averaging over an entire boundary. This result provides preliminary validation of the simplified ablation model when applied to an alternative geometry serving as a foundation for future work.

V. Conclusion

A simplified model quantifying the ablation process in an APPT has been implemented in MACH2 and validated with respect to mass loss per discharge through comparison to the experimental results of two APPT's of differing configuration. Another result of this work was the fabrication of a prototype APPT of novel geometry and its operation at two separate facilities producing comparable results, verifying the experimental data. The current work has also provided insights regarding the time scales of mass loss in an alternative APPT configuration, showing the amount of mass lost from the propellant surface after the current pulse as well as its contribution to the total impulse bit. Although the current model in MACH2

over predicts the impulse bit, the agreement between ablated mass provides confidence in using the current modeling setup to qualitatively explore and optimize alternative APPT configurations. Future work will consist of the inclusion of an upgraded SESAME EOS table which will include a larger range of lower level densities allowing for more accurate characterization the physical processes of this class of thruster as well as the experimental acquisition of impulse bit measurements of the novel prototype APPT presented.

References

[1]Burton, R. L. and Turchi, P. J., "Pulsed Plasma Thruster," *Journal of Propulsion and Power*, Vol. 14, No. 5, 1998, pp. 716–735.

[2]Mikellides, P. G. and Turchi, P. J., "Modeling of late-time ablation in Teflon pulsed plasma thrusters," *32nd AIAA/ASME/SAE/ASEE Joint Propulsion Conference and Exhibit*, Lake Buena Vista, FL, July 1996.

[3]Keefer, D. R. and Rhodes, R., "Electromagnetic Acceleration in Pulsed Plasma Thrusters," *Proceedings of the 25th International Electric Propulsion Conference*, The Electric Rocket Propulsion Society, Worthington, OH, 1997, pp. 229–236.

[4]Cassibry, J. T., Thio, Y. C., Markusic, T. E., and Wu, S. T., "Numerical Modeling of a Pulsed Electromagnetic Plasma Thruster Experiment," *Journal of Propulsion and Power*, Vol. 22, No. 3, 2006, pp. 628–636.

[5]Turchi, P. J., Mikellides, I. G., Mikellides, P. G., and Kamhawi, H., "Optimization of Pulsed Plasma Thrusters for Microsatellite Propulsion," *35th AIAA/ASME/SAE/ASEE Joint Propulsion Conference and Exhibit*, Los Angeles, CA, June 1999.

[6]Mikellides, P. G. and Neilly, C., "Modeling and Performance Analysis of the Pulsed Inductive Thruster," *Journal of Propulsion and Power*, Vol. 23, No. 1, 2007, pp. 51–58.

[7]Turchi, P. J., Davis, J. F., and Roderick, R. F., "MPD Arcjet Thrust Chamber Flow Studies," *AIAA Paper 90-2664*, July 1990.

[8]Holian, K. S., "T-4 Handbook of Material Properties Database. Vol Ic: EOS," La-1160-ms, Los Alamos National Laboratory, Los Alamos, NM, Nov. 1984.

[9]Mikellides, I. G., *Theoretical Modeling and Optimization of Ablation-fed Pulsed Plasma Thrusters*, Ph.D. thesis, Ohio Sate University, 1999.

[10]Henrikson, E. M. and Mikellides, P. G., "Experimental Assessment of a Benchmark Ablation-fed Pulsed Plasma Thruster," *43rd AIAA/ASME/SAE/ASEE Joint Propulsion Conference and Exhibit*, Cincinnati, OH, July 2007.

[11]Turchi, P. J., Mikellides, I. G., Mikellides, P. G., and Kamhawi, H., "Pulsed Plasma Thrusters for Microsatellite Propulsion: Techniques for Optimization," *Micropropulsion for Small Spacecraft*, edited by M. M. Micci and A. D. Ketsdever, Vol. 187 of *Progress in Astronautics and Aeronautics*, AIAA, 2000, p. 356.

[12]Pencil, E. and Kamhawi, H., "Alternate Propellant Evaluation for 100-joule-class Pulsed Plasma Thrusters," *39th AIAA/ASME/SAE/ASEE Joint Propulsion Conference and Exhibit*, Huntsville, AL, July 2003.